Solid-State ^{113}Cd NMR of Three Structural Isomers of $[S_4Cd_{10}(SPh)_{16}]^{4-}$

Garry S. H. Lee,[1] Keith J. Fisher,[1] Anthony M. Vassallo,[2] John V. Hanna,[2] and Ian G. Dance*,[1]

School of Chemistry, University of NSW, Kensington, NSW 2033, Australia, and CSIRO Division of Coal and Energy Technology, P.O. Box 136, North Ryde, NSW 2113, Australia

Received July 9, 1992

Solid-state ^{113}Cd NMR chemical shift (δ_{iso}) and chemical shift anisotropy (δ_{ii}) data are reported for crystalline samples of three different compounds containing the $[S_4Cd_{10}(SPh)_{16}]^{4-}$ cluster. This cluster is a supertetrahedral fragment of the cubic (sphalerite) CdS lattice and contains two types of CdS_4 coordination, $Cd^i\{(\mu_3\text{-}S)_2(\mu\text{-}SPh)_2\}$ and $Cd^o\{(\mu\text{-}SPh)_3(SPh)\}$. Although the Cd sites in these compounds are all pseudotetrahedral, there are in these three different samples small distortions and variations in the coordination geometry at the Cd atoms, arising from configurational isomerism at (μ-SPh) and crystal packing variations at the periphery of the clusters. The chemical shift data reflect these geometrical variations. Chemical shift anisotropies ($\delta_{33} - \delta_{11}$) range from 207 to 480 ppm for the pseudotetrahedral CdS_4 coordination. Variations in the chemical shift data correlate principally with S–Cd–S angle variation. Isotropic chemical shifts for Cd^o vary by only 20 ppm, but individual δ_{ii} and chemical shift anisotropies ($\delta_{33} - \delta_{11}$) are changed by up to 70 ppm for 5° variations in angles at Cd^o. At Cd^i, angle differences of similar magnitude cause δ_{iso} values to vary by 46 ppm, δ_{ii} values by 80 ppm, and ($\delta_{33} - \delta_{11}$) values by 100 ppm. It is postulated that δ_{33} for Cd^i is oriented normal to the S–Cd^i–S plane and is due to the Cd^i–S coordination: the $\delta_{33}(Cd^i)$ range of 807 to 887 ppm is 110–190 ppm greater than δ_{iso} for CdS, an effect which is attributed to the substantial difference in Cd–S bond lengths, 2.48 Å in $[S_4Cd_{10}(SPh)_{16}]^{4-}$ and 2.53–2.55 Å in CdS. The data and correlations reported will be valuable in the interpretation of ^{113}Cd NMR chemical shift data for biological and electronic materials based on cadmium sulfide and thiolate clusters. Crystal structure data for $(Et_3NH)_4[S_4Cd_{10}(SPh)_{16}]$ are reported.

Introduction

There now exists a range of polycadmium systems where the coordination environment is CdS_4. These include the metallothionein proteins, Cd-substituted Zn cysteine proteins (including the zinc finger DNA binding proteins[3]),[4] colloidal CdS used to catalyze photoredox reactions and for optoelectronics,[5] the (γ-glutamylcysteinyl)$_n$glycine oligopeptide (γ-ECG or phytochelatin) complexes with Cd,[6] bionanocrystallites of CdS and γ-ECG peptides,[7] and nonmolecular Cd metal thiolate lattices.[8] The structures of some of these have been determined crystallographically, but others have not yet been crystallized satisfactorily, and some, being heterogeneous samples, are unlikely to be characterized structurally by diffraction methods. Cadmium NMR techniques (usually ^{113}Cd (12.3%) but possibly ^{111}Cd (12.7%), both $I = {}^1/_2$) are valuable for the investigation of these materials,[9] in solution and in solid samples, and provide short-range information while diffraction methods depend on long-range order.

Cadmium chemical shifts δ(Cd) are widely dispersed and very sensitive to small changes in local environments. Measurements in the solid state allow access to additional information,[10] including the magnitude of the anisotropy of the chemical shift tensor, the asymmetry of the tensor, and, from single crystals, the orientation of the chemical shift tensor in the molecular frame.[9a] These solid-state NMR data are also sensitive to the immediate Cd environment and can be valuable in the deployment of Cd NMR in characterization of these materials. The calibration of Cd NMR chemical shift parameters, at the level of resolution required for effective structure elucidation, is largely empirical. In the case of Cd coordinated only by sulfur ligands there are three very different results in the literature. First, the tetrahedrally coordinated Cd in hexagonal CdS has an axial chemical shift anisotropy ($\delta_\parallel - \delta_\perp$) of 54 ppm, with δ_{iso} = 690 ppm[11,12] even though the CdS_4 coordination has virtual T_d symmetry: the axial distortions are only 0.4° from tetrahedral and 0.181 Å in Cd–S

(1) University of New South Wales.
(2) CSIRO Division of Coal and Energy Technology.
(3) (a) Berg, J. M. *Met. Ions Biol. Syst.* **1989**, *25*, 235–254. (b) Berg, J. M. *Prog. Inorg. Chem.* **1989**, *37*, 143. (c) South, T. L.; Kim, B.; Summers, M. F. *J. Am. Chem. Soc.* **1989**, *111*, 395–396.
(4) (a) Armitage, I. M.; Otvos, J. D. *Biochemical Structure Determination by NMR*; Sykes, B. D., Glickson, J., Bothner-By, A. A., Eds.; Marcel Dekker: New York, 1982; Chapter 4. (b) Otvos, J. D.; Olafson, R. W.; Armitage, I. M. *J. Biol. Chem.* **1982**, *257*, 2427. (c) Armitage, I. M.; Boulanger, Y. In *NMR of Newly Accessible Nuclei*; Laszlo, P., Ed.; Academic Press: New York, 1983; Vol. 1, p 157. (d) Summers, M. F. *Coord. Chem. Rev.* **1988**, *86*, 43–134. (e) Giedroc, D. P.; Johnson, B. A.; Armitage, I. M.; Coleman, J. E. *Biochemistry* **1989**, *28*, 2410.
(5) (a) Henglein, A. *Top. Curr. Chem.* **1988**, *143*, 113–175. (b) Henglein, A. *Chem. Rev.* **1989**, *89*, 1861–73. (c) Steigerwald, M. L.; Brus, L. E. *Annu. Rev. Mater. Sci.* **1989**, *19*, 471–95. (d) Steigerwald, M. L.; Brus, L. E. *Acc. Chem. Res.* **1990**, *23*, 183–188. (e) Mau, A. W.-H.; Huang, C.-B.; Katuka, N.; Bard, A. J. *J. Am. Chem. Soc.* **1984**, *106*, 6537–6542. (f) Tricot, Y. M.; Fendler, J. H. *J. Phys. Chem.* **1986**, *90*, 3369–74. (g) Wang, Y.; Herron, N. *J. Phys. Chem.* **1987**, *91*, 257–260. (h) Wang, Y.; Mahler, W.; Herron, N.; Suna, A. *J. Opt. Soc. Am.* **1989**, *B6*, 808–813. (i) Herron, N.; Wang, Y.; Eddy, M. M.; Stucky, G. D.; Cox, D. E.; Moller, K.; Bein, T. *J. Am. Chem. Soc.* **1989**, *111*, 530–540. (j) Herron, N.; Wang, Y.; Eckert, H. *J. Am. Chem. Soc.* **1990**, *112*, 1322–1326. (k) Wang, Y.; Herron, N. *J. Phys. Chem.* **1991**, *95*, 525–532.
(6) Gekeler, W.; Grill, E.; Winnacker, E.-L.; Zenk, M. H. *Z. Naturforsch.* **1989**, *44c*, 361–369.
(7) (a) Reese, R. N.; Winge, D. R. *J. Biol. Chem.* **1988**, *263*, 12832–12835. (b) Dameron, C. T.; Reese, R. N.; Mehra, R. K.; Kortan, A. R.; Carroll, P. J.; Steigerwald, M. L.; Brus, L. E.; Winge, D. R. *Nature* **1989**, *338*, 596–597. (c) Dameron, C. T.; Winge, D. R. *Inorg. Chem.* **1990**, *29*, 1343–1348.
(8) (a) Craig, D. C.; Dance, I. G.; Garbutt, R. G. *Angew. Chem., Int. Ed. Engl.* **1986**, *25*, 165. (b) Dance, I. G.; Garbutt, R. G.; Craig, D. C.; Scudder, M. L.; Bailey, T. D. *J. Chem. Soc., Chem. Commun.* **1987**, 1164–1167. (c) Dance, I. G.; Garbutt, R. G.; Craig, D. C.; Scudder, M. L. *Inorg. Chem.* **1987**, *26*, 4057–4064. (d) Dance, I. G.; Garbutt, R. G.; Bailey, T. D. *Inorg. Chem.* **1990**, *29*, 603–608.
(9) (a) Ellis, P. D. In *The Multinuclear Approach to NMR Spectroscopy*; Lambert, J. B., Riddell, F. G., Eds.; D. Riedel Publishing Co.: Dordrecht, The Netherlands, 1983; Chapter 22, pp 457–523. (b) Summers, M. F. *Coord. Chem. Rev.* **1988**, *86*, 43–134.
(10) (a) Wasylishen, R. E.; Fyfe, C. A. *Annu. Rep. NMR Spectrosc.* **1982**, *12*, 1–80. (b) Fyfe, C. A. *Solid State NMR for Chemists*; CFC Press: Guelph, Canada, 1983.
(11) (a) Nolle, A. *Z. Naturforsch.* **1978**, *33A*, 666–671. (b) Dubois Murphy, P.; Gerstein, B. C. *J. Am. Chem. Soc.* **1981**, *103*, 3282.
(12) All chemical shifts δ in this paper are expressed on the positive frequency scale, relative to 0.1 M aqueous $Cd(NO_3)_2$ as 0: interconversions with the eight other reference scales appearing in the literature are given in the Experimental Section.

0020-1669/93/1332-0066$04.00/0

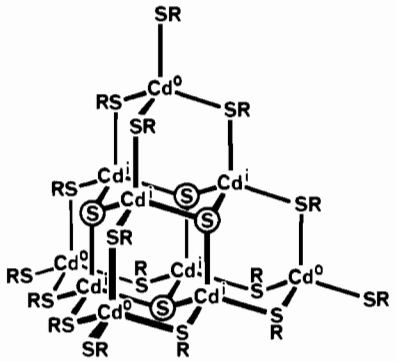

Figure 1. Idealized core structure of $[S_4Cd_{10}(SPh)_{16}]^{4-}$, defining the Cd^i and Cd^o atoms. The circled atoms are S^{2-}.

bond distance.[13] Second, in $[Cd\{1,1\text{-}S_2C_2(CN)_2\}_2]^{2-}$ (which has Cd–S distances of 2.588 (×2), 2.678 (×2), and 2.96 (×2) Å), the chemical shift tensor components are 134, 137, and 504 ppm.[14] Third, and in strong contrast, cadmium coordinated only by three arenethiolate ligands has δ_{iso} = 672 ppm and a nonaxial tensor (994, 549, 473 ppm) when trigonal planar with S–Cd–S angles deviating by 2.5° from 120° but δ_{iso} = 617 ppm and a nonaxial tensor (943, 544, 364 ppm) with similar anisotropy when the coordination is planar but with S–Cd–S angles ranging 101–135°.[15]

On this basis, the assignment of stereochemical details for cadmium coordination by sulfur ligands using chemical shift anisotropy data alone would be ambiguous. In order to develop the technique it is necessary to accumulate Cd NMR data for well-defined and graded systems. In this paper we present such data for three stereochemical isomers of the anion $[S_4Cd_{10}(SPh)_{16}]^{4-}$,[16] which are particularly relevant to the Cd/S/SR systems mentioned above.

The important features of the structure of $[S_4Cd_{10}(SPh)_{16}]^{4-}$ are shown in Figure 1. The 10 Cd atoms and 20 S atoms are congruent with a supertetrahedral fragment of the cubic CdS lattice (sphalerite, zinc blende) and constitute four fused adamantanoid cages. There are six inner (Cd^i) atoms, constituting an octahedron, of which four triangular faces are capped with (μ_3-S) ligands and the other four such faces are capped with (μ-SPh)$_3$Cd(SPh) groups. The four outer Cd^o atoms constitute a tetrahedron. The local coordination of the inner Cd atoms is $\{Cd^i(\mu_3\text{-}S)_2(\mu\text{-}SPh)_2\}$, while that of the outer atoms is $\{(\mu\text{-}SPh)_3Cd^o(SPh)\}$. Each ($\mu$-SPh) ligand is pyramidal at S, and thus has two configurations, yielding a total of 186 configurational isomers for the whole structure,[16] and none of these can adopt the high T_d symmetry possible for the $Cd_{10}S_{20}$ core. In addition to these configurational variables, there are the subtle conformational variables of rotation about the terminal Cd–S bonds and rotation about all S–C bonds. In solution the configurational and conformational changes are very rapid, and the ^{113}Cd NMR spectrum is that of the completely averaged structure with symmetry T_d: the Cd^i and Cd^o resonances occur at 668 and 585 ppm, respectively (at 300 K), with $^2J(Cd^i\text{–}Cd^i)$ and $^2J(Cd^i\text{–}Cd^o)$ coupling resolved.[17]

We have determined three different crystal structures containing the $[S_4Cd_{10}(SPh)_{16}]^{4-}$ cluster, in which these configurational and conformational variations are trapped. These compounds provide subtle modifications of the Cd environments and therefore are valuable in the empirical calibration of ^{113}Cd chemical shifts and anisotropies. The relevant configurational isomerism is presented in Figure 2, in terms of the directions of the S–C vectors of the (μ-SPh)$_{12}$ ligands, relative to the truncated tetrahedron constituted by their 12 S atoms.[16]

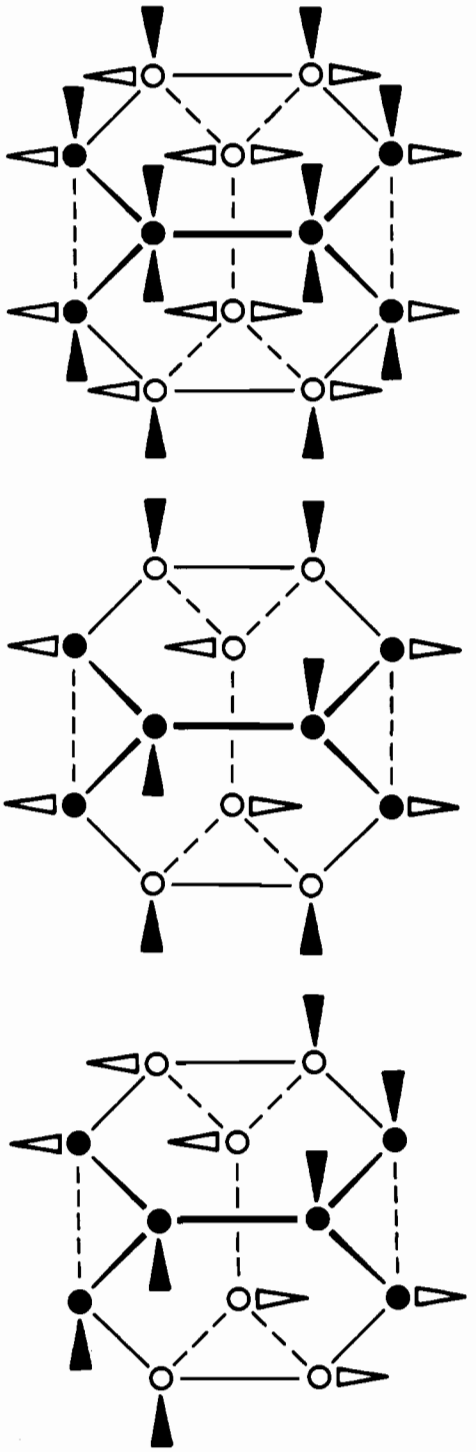

Figure 2. Thiolate substituent configurations in $[S_4Cd_{10}(SPh)_{16}]^{4-}$: (a, top) Diagrammatic representation of the two possible substituent orientations at each of the 12 doubly bridging thiolate S atoms (circles) which constitute a truncated tetrahedron, where full lines and filled circles represent positions above the centroid plane; (b, middle) orientations of the Ph substituents in the S_4 ($\bar{4}$) configurational isomer which occurs in **1**; (c, bottom) orientations of the Ph substituents in the different S_4 ($\bar{4}$) configurational isomer which occurs in **2** and **3**.

Sample **1** is $(Me_4N)_4[S_4Cd_{10}(SPh)_{16}]$ crystallized as needles from DMF/H_2O and contains the configurational isomer b shown in Figure 2, while sample **2** is a different crystalline modification of $(Me_4N)_4[S_4Cd_{10}(SPh)_{16}]$ obtained from acetonitrile, containing the configurational isomer c of Figure 2. Sample **3** is $(Et_3NH)_4[S_4Cd_{10}(SPh)_{16}]$, containing the same configurational isomer c as **2** but with hydrogen bonds between the four surrounding

(13) Mair, S. L.; Barnea, Z. *Acta Crystallogr.* **1975**, *A31*, 201–207.
(14) Li, H. Y.; Amma, E. L. *Inorg. Chim. Acta* **1990**, *177*, 5–7.
(15) Santos, R. A.; Gruff, E. S.; Koch, S. A.; Harbison, G. S. *J. Am. Chem. Soc.* **1991**, *113*, 469–475.
(16) Dance, I. G.; Choy, A.; Scudder, M. L. *J. Am. Chem. Soc.* **1984**, *106*, 6285–6295.
(17) Dance, I. G. *Aust. J. Chem.* **1985**, *38*, 1745.

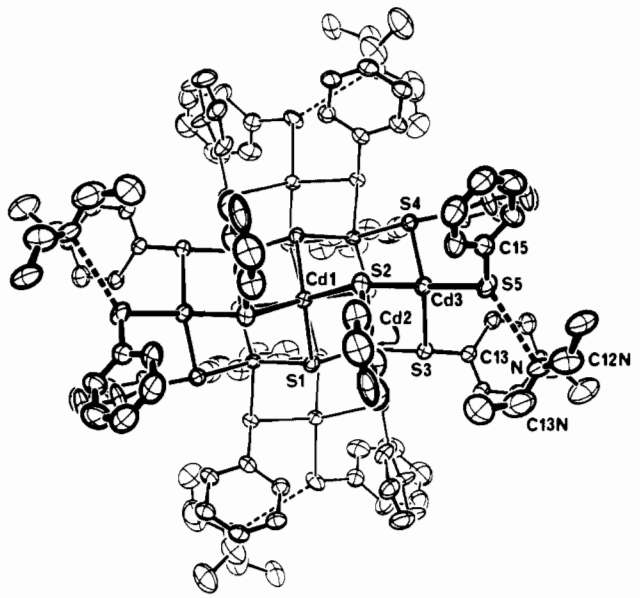

Figure 3. Anion and associated cation in $(Et_3NH)_4[S_4Cd_{10}(SPh)_{16}]$ (**3**) with $\bar{4}$ point symmetry. The NH–S hydrogen bonds are marked as broken lines. Atoms of the asymmetric unit are labeled, and ellipsoids are drawn to include 15% electron density.

Table I. Bond Distances (Å) and Angles (deg) for Cd^o in **1–3**

	1	**2**	**3**
Cd^o–S^t	2.486	2.459	2.447
Cd^o–S^b	2.559	2.557	2.548
Cd^o–S^b	2.567	2.557	2.548
Cd^o–S^b	2.568	2.584	2.558
S^t–Cd^o–S^b	104.5	109.6	103.6
S^t–Cd^o–S^b	112.1	111.7	113.6
S^t–Cd^o–S^b	121.4	113.2	115.9
S^b–Cd^o–S^b	100.3	101.4	95.2
S^b–Cd^o–S^b	104.1	105.1	110.2
S^b–Cd^o–S^b	114.7	115.6	119.0

ammonium cations and the S atoms of the terminal thiolate ligands, with concomitant further distortion of the cluster structure. The stereochemical variations which occur at the surface of each cluster have consequences for geometry for the core: there are distortions of the core, and the idealized tetrahedral stereochemistry at each Cd atom no longer obtains. In each crystal the $[S_4Cd_{10}(SPh)_{16}]$ cluster has S_4 ($\bar{4}$) molecular symmetry, which means that the $(Cd^i)_6$ core atoms are of two kinds, axial (×2) and equatorial (×4) with respect to the unique $\bar{4}$ axis, labeled Cd^i_{ax} and Cd^i_{eq}, respectively. The four Cd^o atoms in each structure are equivalent. Therefore the solid-state NMR of these three compounds are not too complex for straightforward interpretation and yet reveal the effects of three different types of geometrical distortion at two chemically different types of CdS_4 coordination environment.

Results

Crystal Structures. The crystal structures of **1** and **2** have been reported in detail.[16] The crystal structure of **3** is similar but contains a hydrogen bond between the tertiary ammonium cation and the sulfur atom of the terminal thiolate ligand, as shown in Figure 3. This hydrogen bond, of length N- -S5 = 3.30 (1) Å, does not elongate the Cd–S^t bond, which is in fact shorter in **3** than in **1** and **2**. Molecular dimensions are included in Tables I and II, while fuller details are provided in the Experimental Section and in the supplementary material:[18] S^t = terminal SPh, S^b = bridging SPh.

NMR Data. The CP MAS spectra of **1–3** recorded at 2.3 T are shown in Figure 4, and the δ_{iso} values are recorded in Table III.[19] In all three compounds there is one line for Cd^o, as required

(18) See paragraph at end of paper regarding supplementary material.

Table II. Bond Distances (Å) and Angles (deg) for Cd^i in **1–3**

	1		**2**		**3**	
	Cd^i_{ax}	Cd^i_{eq}	Cd^i_{ax}	Cd^i_{eq}	Cd^i_{ax}	Cd^i_{eq}
Cd–S^{2-}	2.485	2.475	2.472	2.477	2.488	2.448
Cd–S^{2-}	2.485	2.504	2.472	2.489	2.488	2.494
Cd–SR	2.600	2.612	2.612	2.590	2.596	2.565
Cd–SR	2.600	2.627	2.612	2.606	2.596	2.611
S^{2-}–Cd–S^{2-}	125.0	124.1	123.5	125.9	123.2	125.8
RS–Cd–SR	98.1	104.6	102.1	101.7	100.5	104.0
S^{2-}–Cd–SR	107.3	97.3	106.6	100.6	102.5	98.1
S^{2-}–Cd–SR	107.3	99.3	106.6	102.1	102.5	99.2
S^{2-}–Cd–SR	107.9	111.6	108.0	111.7	113.1	113.6
S^{2-}–Cd–SR	107.9	116.9	108.0	112.6	113.1	114.9

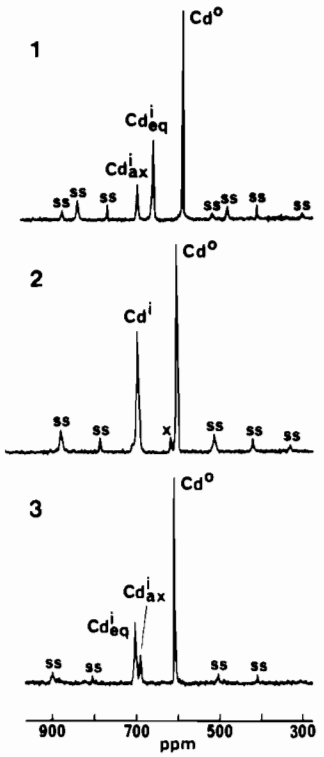

Figure 4. ^{113}Cd CP-MAS NMR spectra of **1–3** measured at 2.3 T, 300 K. The Cd^o, Cd^i_{eq}, and Cd^i_{ax} labels are explained in the text. Peaks labeled ss are spinning sidebands. The small peak marked × in the spectrum of **2** is an impurity.

by the crystal structures, with $\delta(Cd^o)$ values ranging from 588 to 609 ppm, 3–24 ppm larger than the value in solution. However the three compounds differ in their Cd^i resonances: in **2** there is only one Cd^i resonance resolved, whereas in **1** and **3** the Cd^i_{ax} and Cd^i_{eq} resonances are resolved (see Table III). The integrated intensities of the lines in these spectra are in fair agreement with the expected ratios 4:2:4 for Cd^o:Cd^i_{ax}:Cd^i_{eq}, with no ambiguity in the assignments of Cd^i_{ax} and Cd^i_{eq}: the variations from the ideal intensity ratios arise because T_1 values are large and spectra were acquired under conditions of incomplete relaxation.

The isotropic chemical shifts for the Cd^i_{ax} atoms show very little dependence on crystal structure and are about 20 ppm upfrequency of the resonance of Cd^i_{ax} in solution. In **1** the Cd^i_{eq} resonance is 36 ppm negative of Cd^i_{ax}; in **2** the two resonances are not resolved (i.e. they are separated by less than 3 ppm[20]), while in **3** the Cd^i_{eq} resonance is 14 ppm positive of Cd^i_{ax}.

The CP MAS spectra recorded at 9.4 T are shown in Figure 5. The chemical shift anisotropies of all resonances for the three

(19) Throughout this paper we use the symbols δ and δ_{ii} for chemical shifts and the principal elements of the chemical *shift* tensor, all defined in frequency units, and avoid the symbols σ and σ_{ii} which have been used incorrectly and misleadingly in recent solid-state NMR literature to represent *both* frequency chemical shifts and magnetic shielding.

(20) The line widths and limit of resolution for these compounds are 100–200 Hz: this is not a consequence of magnetic inhomogeneity, because the $3CdSO_4{\cdot}8H_2O$ reference line has a line width of 15 Hz.

Table III. Chemical Shifts and Anisotropies, with δ_{ii} Values in ppm Frequency Units, Referenced to 0.1 M aqueous $Cd(NO_3)_2$

compd	atom	δ_{11}[a]	δ_{22}[a]	δ_{33}[a]	δ_{iso}^{calc}	δ_{iso}^{obs}	$\delta_{33}-\delta_{11}$	η
1	Cd^o	447	592	727	589	588	280	0.96
	Cd^i_{eq}	427	768	807	667	658	380	0.21
	Cd^i_{ax}	427	767	837	677	694	410	0.34
2	Cd^o	452	637	722	604	604	270	0.63
	Cd^i[b]	418	782	882	694	696	464	0.43
3	Cd^o	502	623	709	611	609	207	0.83
	Cd^i_{eq}	407	798	887	697	704	480	0.37
	Cd^i_{ax}	447	757	867	690	690	420	0.52

[a] Estimated uncertainties are ±20 ppm. [b] The resonances for Cd^i_{ax} and Cd^i_{eq} are not resolved for **2**.

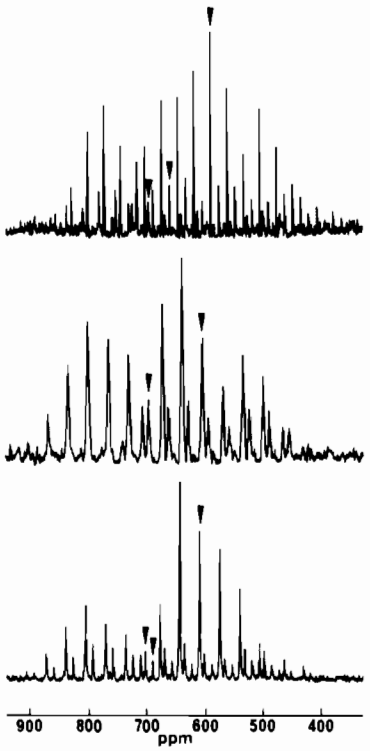

Figure 5. ^{113}Cd CP-MAS NMR spectra of **1**–**3** measured at 9.4 T, 300 K. The centerband peaks are marked.

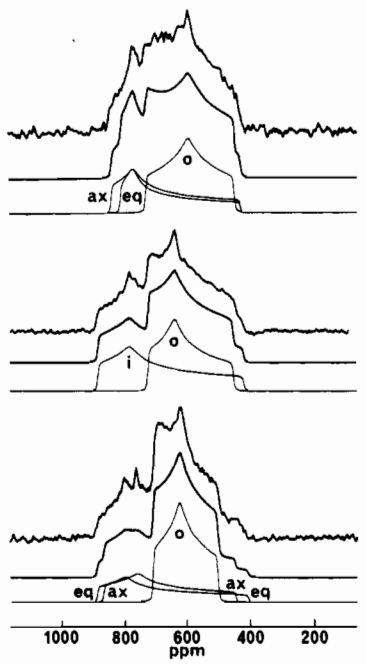

Figure 6. Static ^{113}Cd NMR powder spectra for **1** (top), **2** (middle), and **3** (bottom). For each compound the upper trace is the spectrum recorded at 88.7 MHz, the center trace is the calculated powder spectrum, and the lower traces are the calculated components for Co^o, Cd^i_{eq}, and Cd^i_{ax}.

compounds have been determined by analysis of the intensities of the combs of spinning side bands obtained at various MAS spinning speeds, using Herzfeld–Berger analysis,[21] and refined by fitting to the absorption envelopes in the static spectra. The calculated and observed static spectra for **1**–**3** are shown in Figure 6, and the principal components of the anisotropy tensor are presented in Table III.[19] We list also the maximum chemical shift anisotropy, $(\delta_{33}-\delta_{11})$, and the asymmetry η ($\eta = 1-|\rho|$, where $\rho = (\delta_{33}-2\delta_{22}+\delta_{11})/(\delta_{33}-\delta_{11})$[22]), which is a measure of the differentiation of the tensor principal components: δ_{22} is midway between δ_{33} and δ_{11} at $\eta = 1$, while at $\eta = 0$ the tensor has axial symmetry with δ_{22} equal to δ_{33} or δ_{11}.

From the data in Table III we note the following comparisons and significant differences between the three sites and between the three compounds. (i) The Cd^o sites are less anisotropic than Cd^i sites. The $(\delta_{33}-\delta_{11})$ values range 207–280 ppm for Cd^o but 380–480 for Cd^i: $\delta_{11}(Cd^i) < \delta_{11}(Cd^o)$; $\delta_{33}(Cd^i) > \delta_{33}(Cd^o)$. (ii) The Cd^o sites are less axially symmetric (larger η) than the Cd^i sites. (iii) At Cd^o, the compound dependence occurs mainly in δ_{11} and δ_{22}: $\delta_{11}(Cd^o)$ in **3** is at least 50 ppm larger than in the other two compounds. (iv) It is possible to trace the origins of the differences and reversals in the δ_{iso} values for Cd^i_{ax} and Cd^i_{eq} in the three samples. For Cd^i in both **1** and **3** it is mainly the δ_{33} values which show the greatest variation and which differentiate the Cd^i_{ax} and Cd^i_{eq} sites: in **3** δ_{33} Cd^i_{eq} (887) > δ_{33} Cd^i_{ax} (867), while in **1** δ_{33} Cd^i_{eq} (807) < δ_{33} Cd^i_{ax} (837).

Part of the lesser anisotropy and greater asymmetry of Cd^o compared with Cd^i is attributable to the chemical differences in the coordination environments, namely $\{Cd^o(\mu\text{-SPh})_3(SPh)\}$ and $\{Cd^i(\mu_3\text{-S})_2(\mu\text{-SPh})_2\}$, but there are also geometrical differences which are analyzed in the following section.

Structural Data. At its highest level of idealization the $Cd_{10}S_{20}$ core has all bonds of equal length and all angles are 109.5°. There are two distorting influences. One distortion is a consequence of the five chemically different functionalities, Cd^o, Cd^i, $(\mu_3\text{-}S^{2-})$, bridging PhS^- (S^b), and terminal PhS^- (S^t), and consequent bond length differences. Both Cd^o and Cd^i have two types of bonds which differ in length by about 0.1 Å: the Cd^i–S^{2-} bond length, averaging 2.48 Å over all Cd atoms, is similar in length to Cd^o–S^t (mean 2.464 Å), while Cd^o–S^b (mean 2.56 Å) is close to Cd^i–S^b (mean 2.60 Å). At Cd^o there is one shorter and three longer bonds, while at Cd^i there are two of each length. The second distortion is a consequence of the different configurations and conformations of the phenyl rings and the hydrogen bonding in **3**.

Figure 7 shows the global structural features of the three clusters, in comparison with the core geometry as idealized when subject only to the differences in bond distances. The differing orientations of the phenyl substituents clearly are associated with distortions of the framework and affect details of the $Cd_{10}S_{20}$ geometry. The main observations are that the distortion of the $Cd_{10}S_{20}$ core is larger in **1** and **3** than in **2** and that in **3** there is a substantial twisting of the framework about the $\bar{4}$ axis. This twisting of **3** is in the direction of the hydrogen bond between S^t and the Et_3NH^+ cation, shown in more detail in Figure 3: this hydrogen bond does not weaken the Cd–S^t bond, which is shortest

(21) Herzfeld, J.; Berger, A. E. *J. Chem. Phys.* **1980**, *73*, 6021–6030.
(22) Carty, A. J.; Fyfe, C. A.; Lettinga, M.; Johnson, S.; Randall, L. H. *Inorg. Chem.* **1989**, *28*, 4120–4124.

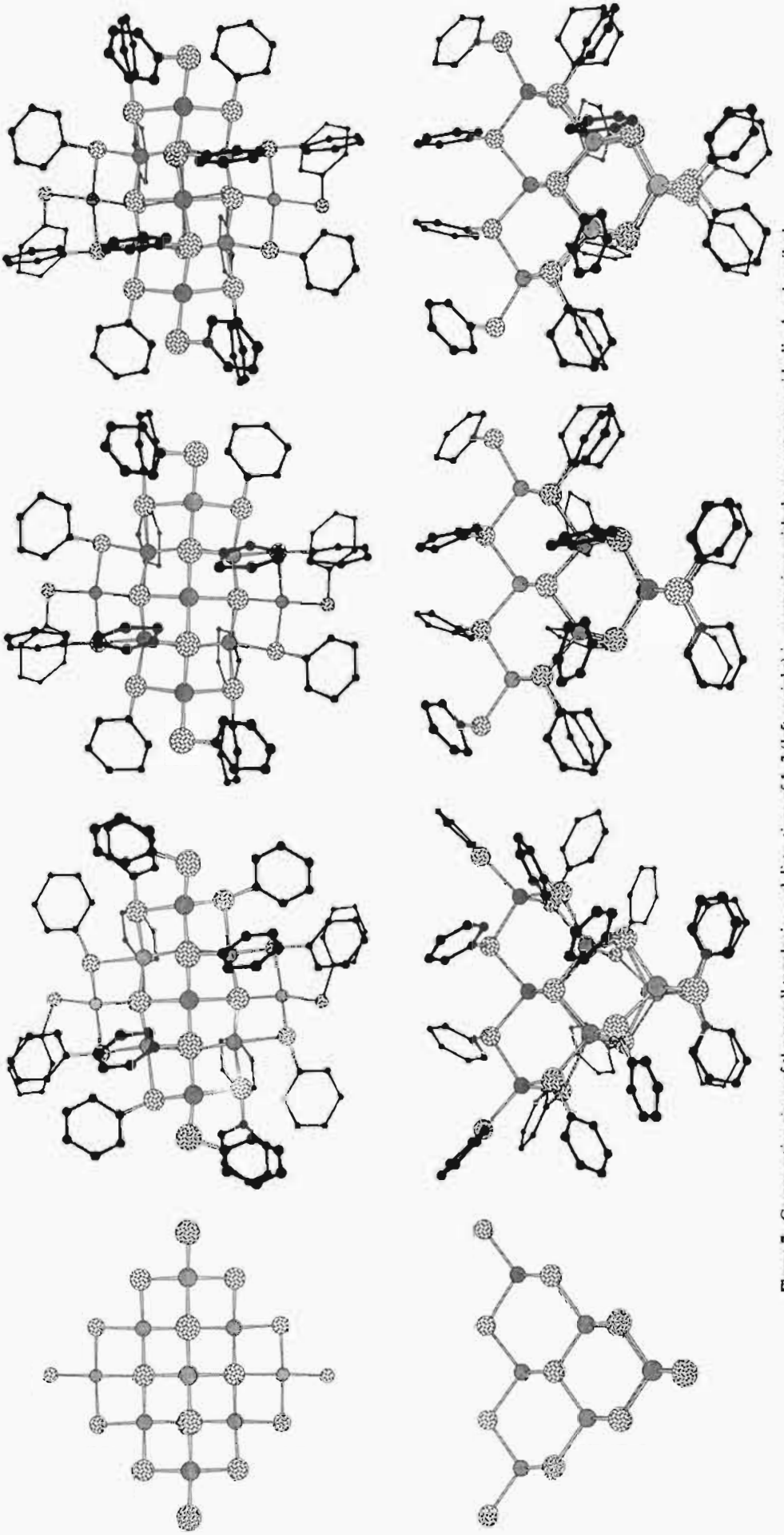

Figure 7. Comparative views of the overall topologies and distortions of **1**–**3** (left to right) in comparison with the core structure idealized as described in the text. The upper and lower views are axial and equatorial relative to the 4 axis.

Table IV. Comparative Measurements of ^{113}Cd Chemical Shifts (ppm) for Cd Chemical Shift Reference Compounds, Solid and Liquid

CdS(s)	$CdMe_2$(liq)	$Cd(ClO_4)_2$(aq) (infinite dilution)	$Cd(ClO_4)_2$(aq) (0.1 M)	$Cd(NO_3)_2$(aq) (0.1 M)	$Cd(ClO_4)_2 \cdot 6H_2O$(s) (same as $Cd(ClO_4)_2$(aq), 0.1 M, I = 4.5)	$3CdSO_4 \cdot 8H_2O$(s)		$Cd(NO_3)_2 \cdot 4H_2O$(s)	ref
808						56.4	43.6	0	11b[a]
						53	40	0	*b*[a]
					105			0	29[a]
					0	−45	−58	−100	32[a]
		5	3.7	0		−60.9	−73.5		*c*, *d*
	643		0						33
42.3	0								5j

[a] We have reversed the sign of the chemical shifts quoted by these authors, to be consistent with our data. [b] Cheung, T. T. P.; Worthington, L. E.; Dubois Murphy, P.; Gerstein, B. C. *J. Magn. Reson.* **1980**, *41*, 158. [c] This work. [d] Borzo, M.; Maciel, G. E. *J. Chem. Soc., Chem. Commun.* **1973**, 394.

in **3**. However, close comparative inspection of the undistorted and actual structures in Figure 7 reveals many angular variations that can be correlated with (i) the configurational difference in which the eight PhS^b ligands equatorial to the $\bar{4}$ axis remain in an equatorial girdle in **2** and **3**, but not in **1**, (ii) the conformation of the PhS^t ligand in **1**, which differs from that in **2** and **3**, and (iii) the hydrogen bond to the cation in **3**. We do not attribute the core distortions to specific *intra*molecular Ph–Ph interactions, because *inter*molecular Ph–Ph interactions are also significant in these crystal structures.[23]

The geometrical data presented in Table I and II are used to interpret the chemical shift tensors: the crystallographic estimated standard deviations for these dimensions are ca. 0.003 Å for M–S and ca. 0.1° for S–M–S: on this basis, differences of >0.02 Å (M–S) and >1° (S–M–S) in tabulated values are significant.

Geometrical Anisotropy and Chemical Shift Anisotropy. At Cd^o the differences in the δ components are that δ_{11} in **3** is at least 50 ppm larger than in the other two and δ_{22} in **1** is at least 30 ppm smaller than in the other two compounds. The Cd^o atoms in all three compounds have similar differentiation of Cd^o–S distances, with 3-fold symmetry, and the compound-dependent δ components do not appear to be a consequence of unusual Cd^o–S bond distances. However there are correlations with angular variations. Cd^o in **2** has the least angular distortion superimposed on the 3-fold distance distortion and has the tensor with the smallest η value (0.63). Although the most axial Cd^o tensor for the three compounds, it still indicates that the small distance and angle distortions from exact 3-fold symmetry have appreciable influences on δ. This is reinforced in **1** and **3**, which have larger and different angular distortions (an anomalously large S^t–Cd^o–S^b angle of 121° in **1** and S^b–Cd^o–S^b angles ranging 95–119° in **3**) superimposed on the distance distortion and more rhombic tensors. The orientation of the Cd^o tensor for each compound is needed to complete the correlation with the distorted geometry.

For the Cd^i atoms several comments can be made about the relationships between chemical shift anisotropy and geometrical distortions. All of the Cd^i atoms possess one large S^{2-}–Cd–S^{2-} angle of 125 ± 1°, which probably contributes much of the anisotropy they display, but it is not possible to distinguish the geometric and electronic contributions to the anisotropy by the S^{2-} ligands. The atom with the largest variability of the four Cd–S distances, Cd^i_{eq} in **3**, has the largest value of $(\delta_{33} - \delta_{11})$, but beyond that there is no generally consistent correlation between Cd^i–S bond lengths and the chemical shift anisotropy. However, it is clearly possible to rationalize the lack of resolution of the Cd^i_{eq} and Cd^i_{ax} resonances in **2** because their distributions of Cd–S distances and angles are very similar. On the other hand, these two sites display the least deviation of S–Cd–S angles from the tetrahedral ideal and yet have one of the largest values of $(\delta_{33} - \delta_{11})$.

Discussion

Measurements of the orientation of the chemical shift anisotropy tensors in the molecular frame are required for fuller interpretation of the data in chemical terms. Nevertheless, the orientations of the Cd^i tensors can be postulated, using data from the literature. The single-crystal ^{113}Cd NMR spectroscopy[24] of $[Cd(S\text{-}2,4,6\text{-}Pr^i_3\text{-}C_6H_2)_2(2,2'\text{-bipyridine})]$ (**4**), which has tetrahedral coordination distorted by the restricted bite of the bipy ligand, reveals that the highest chemical shift tensor component, 815 ppm, is almost perpendicular to the S–Cd–S coordination plane, and the smallest element of the chemical shift tensor is almost perpendicular to the N–Cd–N plane. This result confirms the general observation[25] that the chemical shift effects are manifest in the direction normal to the influential bonds.

The Cd^i atoms in **1**–**3** are comparable with the cadmium atom in **4**, in that they have a pronounced 2-fold overlay in their $\{Cd^i(\mu_3\text{-}S)_2(\mu\text{-}SPh)_2\}$ coordination, with clear differentiation of the Cd–S^{2-} and Cd–SPh distances and an invariant S^{2-}–Cd–S^{2-} angle of 124.5 ± 1°. The S–Cd–S angle of **4** is similarly large, 126°. Combining these data with the observation that δ_{33} is similarly high for all Cd^i, and the fact that S^{2-} is now well-established as causing larger chemical shifts than SPh,[26] and noting the tensor orientation in **4**, we postulate that the δ_{33} component for Cd^i in **1**–**3** is perpendicular to the S^{2-}–Cd^i–S^{2-} plane. We note further similarities between the $\delta(Cd^i)$ tensor components in our $[S_4Cd_{10}(SPh)_{16}]^{4-}$ compounds and in **4** (for which η = 0.16), namely that δ_{22} is appreciably closer to δ_{33} than δ_{11}. Therefore, δ_{11} for the $[S_4Cd_{10}(SPh)_{16}]^{4-}$ compounds is likely to be approximately perpendicular to the $(\mu\text{-SPh})$–Cd^i–$(\mu\text{-SPh})$ plane.

The core of the $[S_4Cd_{10}(SPh)_{16}]^{4-}$ clusters represents a fragment of the CdS lattice. Herron, Wang, and Eckert[5j] report that hexagonal CdS resonates at 42.3 ppm relative to liquid $CdMe_2$, while Look[27] is quoted in Harris and Mann[28] as reporting CdS at 60 ppm relative to $CdMe_2$. Kurtz et al.[29] quote CdS as resonating at −808 ± 5 ppm relative to solid $Cd(NO_3)_2(H_2O)_4$. These data, plus the various reference data displayed comparatively in Table IV, lead to the conclusion that CdS resonates at 685–700 ppm on the scale used in this paper. It is significant that δ_{33} for Cd^i, attributed to the S^{2-}–Cd–S^{2-} coordination, is substantially larger than this, at ca. 860 ppm. This difference is a consequence of the different Cd–S^{2-} distances in the two systems, namely 2.481 Å in the $[S_4Cd_{10}(SPh)_{16}]^{4-}$ compounds compared with 2.526 and 2.548 Å in hexagonal CdS.[13] In the broad view the characteristics of CdS and of the $\{Cd^i(\mu_3\text{-}S)_2(\mu\text{-}SPh)_2\}$ sites of $[S_4Cd_{10}(SPh)_{16}]^{4-}$ are similar, in that the mean Cd chemical shifts are the same (690 ± 15 ppm) and the mean Cd–S distances are the same (2.54 ± 0.01 Å).

The axial anisotropy of the Cd site in hexagonal CdS is 54 ppm. In this context, the substantial and variable anisotropies of the Cd^o and Cd^i sites in $[S_4Cd_{10}SPh)_{16}]^{4-}$ indicate the sensitivity

(23) There can be significant attractive interactions between the phenyl substituents on the periphery of $M_x(SPh)_y$ complexes: Gizachew, D.; Dance, I. G. In preparation.

(24) Santos, R. A.; Gruff, E. S.; Koch, S. A.; Harbison, G. S. *J. Am. Chem. Soc.* **1990**, *112*, 9257–9263.
(25) Rivera, E.; Kennedy, M. A.; Adams, R. D.; Ellis, P. D. *J. Am. Chem. Soc.* **1990**, *112*, 1400–1407 and references contained therein.
(26) (a) Lee, G. S. H. Ph.D. Thesis, UNSW, 1991. (b) Lee, G. S. H.; Dance, I. G. To be published.
(27) Look, D. C. *Phys. Status Solidi B* **1972**, *50*, K97.
(28) Harris, R. K.; Mann, B. E. *NMR and the Periodic Table*; Academic Press: London, 1978; p 265.
(29) Dubois Murphy, P.; Stevens, W. C.; Cheung, T. T. P.; Lacelle, S.; Gerstein, B. C.; Kurtz, D. M., Jr. *J. Am. Chem. Soc.* **1981**, *103*, 4400–4405.

Table V. Numerical Details of the Solution and Refinement of $(Et_3NH)_4[S_4Cd_{10}(SPh)_{16}]$

chem formula	$C_{120}H_{144}Cd_{10}S_{20}N_4$	fw	3407.8
a, b	20.007 (3) Å	space group	$P\bar{4}2_1c$ (No. 114)
c	17.982 (3) Å	T	21 (1) °C
V	7198 (1) Å^3	λ	0.7107 Å
Z	2	ρ_{calc}	1.57 g cm^{-3}
μ	18.3 cm^{-1}	transm coeff	0.998–0.974
$R(F_o)^a$	0.036	$R_w(F_o)^a$	0.028

^{a} $R = \sum^m|\Delta F|/\sum^m|F_o|$; $R_w = [\sum^m w|\Delta F|^2/\sum^m w|F_o|^2]^{1/2}$.

of the Cd chemical shift to electronic and geometrical irregularities in the CdS_4 coordination. At Cd^i in $[S_4Cd_{10}SPh)_{16}]^{4-}$ there are electronic and geometrical contributions to the chemical shift anisotropy, while at Cd^o the anisotropy is mainly geometrical in origin.

In summary, we have demonstrated the sensitivity of the chemical shift anisotropy measured for the solid state to subtle variations in the coordination of cadmium coordinated tetrahedrally by sulfide and thiolate ligands and provided reference data valuable for the interpretation of the solid-state Cd NMR of similar materials and biomolecules with unknown local structure.

Experimental Section

Synthesis. Solvents and reagents were used as received and were not further purified except for Et_3N, which was distilled from KOH/NaOH. All manipulations were carried out under an inert atmosphere of dinitrogen.

Several methods of preparation of $(Q)_4[S_4Cd_{10}(SPh)_{16}]$ ($Q = Me_4N^+$, Et_3NH^+) have been used, including the published method.[16,26a] The self-assembly method outlined here has been used extensively for the preparation of other derivatives of $[S_4Cd_{10}(SPh)_{16}]^{4-}$.

$(Et_3NH)_4[S_4Cd_{10}(SPh)_{16}]$. A solution of $Cd(NO_3)_2{\cdot}4H_2O$ (10 g; 32.4 mmol) dissolved in acetonitrile (20 mL) was added to a solution of PhSH (8.9 g; 80.8 mmol) and Et_3N (8.2 g; 80.8 mmol) in acetonitrile (30 mL). A white precipitate formed on the addition of the Cd^{2+} solution redissolved with stirring. A clear colorless solution remained. Sulfur powder (0.31 g; 9.7 mmol) was added in one portion and dissolved to give a yellow solution. The white solid which deposited after stirring for 10 min was collected, washed with acetonitrile, and vacuum dried. Yield: 6.52 g (82%).

This crude material (3 g) was redissolved in hot acetonitrile (approximately 20 mL), and the solution was left to cool. Colorless block crystals grew within 10 h at room temperature. They were filtered out, washed with cold acetonitrile, and vacuum dried.

^{113}Cd NMR of this solid in solution in DMF confirmed that it contained only the $[S_4Cd_{10}(SPh)_{16}]^{4-}$ anion, and the solid was confirmed as the Et_3NH^+ salt by elemental analysis and single-crystal X-ray structure determination. Anal. Found: C, 42.13; H, 4.18; N, 1.85; Cd, 32.85. Calcd for $C_{120}H_{144}N_4Cd_{10}S_{20}$: C, 42.29; H, 4.27; N, 1.64; Cd, 32.99.

Crystal Structure Determination. The diffraction data were measured using a Enraf-Nonius CAD4 diffractometer: procedures were as previously reported,[30] and numerical details are provided in Table V. The positions of the Cd and S atoms were determined using direct methods (MULTAN), and subsequent Fourier syntheses located the remaining non-hydrogen atoms of the phenyl rings and of the counterion. Refinement was carried out using the program RAELS, with rigid groups including hydrogen atoms for the phenyl rings. The Cd and S atoms, and the atoms of the Et_3NH^+ ion, were refined with anisotropic temperature parameters. The thermal parameters of the phenyl rings were described by a 12-parameter TL model (where T is the translation tensor and L is the libration tensor), with the origin of libration of each phenyl ring fixed on the appropriate S atom. Hydrogen atoms on the counterion (including that of the hydrogen bond from N to S5) were included in calculated positions, assigned thermal parameters equal to those of the atom to which they were bound, and not refined. Anomalous scattering was included for Cd, S, C, and N. Refinement converged with $R = 0.036$ (0.038 for the other enantiomer). The final difference map contained peaks up to 1.4 e Å^{-3} in the vicinity of the Cd atoms, of unknown origin.

The structure is shown in detail in Figure 3, with anisotropic thermal ellipsoids, including the hydrogen bond (N- -S5 = 3.30 (1) Å) between the cation and the terminal thiolate ligand. Atomic parameters and additional dimensions are included in the supplementary material.[18]

NMR Spectroscopy. Solid-state ^{113}Cd NMR spectra were obtained on Bruker CXP-90 and Bruker MSL-400 spectrometers operating at the ^{113}Cd frequency of 19.964 or 88.741 MHz, respectively. Spectra were obtained using conventional ^1H cross-polarization techniques with a contact time of 5 ms and a recycle delay of 5–20s. A ^1H 90° pulse width of 3.75 μs was employed at both fields, with high-power ^1H decoupling being applied during data acquisition periods. Because of the long ^1H T_1 relaxation times for these compounds, complete relaxation between pulses was not achieved. Consequently, the relative intensities of the peaks do not accurately reflect the relative proportions of cadmium sites.

Magic angle spinning (MAS) with spinning speeds of 2.5–5 kHz was used on both spectrometers, but due to the large chemical shift anisotropy encountered at 88.7 MHz, spinning sidebands could not be eliminated at this higher frequency. Samples of approximately 300 mg were spun in 7-mm double air-bearing systems using zirconia rotors.

Free induction decays were collected in 2K data points and zero filled to 4K data points prior to Fourier transformation, and exponential multiplication with a line broadening factor of 10 Hz was employed at both fields. A sweep width of 30 kHz was used, and between 500 and 20 000 scans were needed for an adequate signal.

Static (powder) spectra were obtained at 88.741 MHz over a spectral width of 100 kHz, using a solid-state spin-echo experiment employing a cross-polarization preparation of magnetization and an extended phase cycle.[31] Free induction decays were obtained in 256 data points and zero filled to 1K data points prior to Fourier transformation. An exponential multiplication factor of 200 Hz was used in signal-to-noise enhancement.

Chemical shifts are referenced to the high-field resonance of external crystalline $3CdSO_4{\cdot}8H_2O$.[11b] This very sharp resonance in this nonhygroscopic and stable crystalline compound provides the best practical reference. We measure this resonance at −73.5 ppm relative to a 0.1 M aqueous solution of $Cd(NO_3)_2$ located directly in the solids probe. There are eight different samples that have been used as reference in the reporting of Cd chemical shifts for solid samples, and interconversion between them are not always direct. In Table IV we summarize the principal comparative measurements. Apart from the value of aqueous $Cd(ClO_4)_2$, 0.1 M, $I = 4.5$,[32] there is internal consistency in these data: thus δ(CdS(s)) is measured as 764 ppm relative to the high-field line of 3 $CdSO_4{\cdot}8H_2O$ in ref 11b and calculates through the data in this work and refs 5j, 32, and 33 at 762 ppm.

Chemical shift anisotropies for each resonance were determined by a Herzfeld–Berger analysis[21] of the intensities of the sidebands at various MAS spinning speeds. The values of δ_{11}, δ_{22}, and δ_{33} obtained this way were refined by empirical fitting of the calculated static spectrum to the observed absorption envelope, using the program TENSOR.[34] Estimates of the errors in the tensor components were obtained from this fitting and are given in Table I. The incomplete relaxation due to the long T_1 values does not affect the determinations of the chemical shift tensors.

Acknowledgment. This research is supported by the Australian Research Council, an Australian Postgraduate Award (G.S.H.L.), and a National Research Fellowship (K.J.F.). We acknowledge the assistance of Dr. C. Kennard in collection of the diffraction data and D. C. Craig and Dr. M. L. Scudder for the structure analysis.

Supplementary Material Available: Tables of crystallographic data, crystal structure parameters, and bond lengths and angles for $(Et_3NH)_4[S_4Cd_{10}(SPh)_{16}]$ (5 pages). Ordering information is given on any current masthead page.

(30) Banda, R. M. H.; Dance, I. G.; Bailey, T. D.; Craig, D. C.; Scudder, M. L. *Inorg. Chem.* **1989**, *28*, 1862–1871.

(31) Kunwar, A. C.; Turner, G. L.; Oldfield, E. *J. Magn. Reson.* **1986**, *69*, 124–127.

(32) Mennitt, G.; Shatlock, M. P.; Bartuska, V. J.; Maciel, G. E. *J. Phys. Chem.* **1981**, *85*, 2087–2091.

(33) Howard, J. W., Jr.; Odom, J. D.; Ellis, P. D.; Cardin, A. D. *J. Am. Chem. Soc.* **1975**, *97*, 1672.

(34) Bruker Abacus Library, program no. ABA069.